

ORIGINAL ARTICLE

# Co-Seeding Human Endothelial Cells with Human-Induced Pluripotent Stem Cell-Derived Mesenchymal Stem Cells on Calcium Phosphate Scaffold Enhances Osteogenesis and Vascularization in Rats

Xian Liu, DDS, PhD,<sup>1,2</sup> Wenchuan Chen, DDS, PhD,<sup>1,2</sup> Chi Zhang, DDS,<sup>1,2</sup> Wahwah Thein-Han, PhD,<sup>2</sup> Kevin Hu, DDS,<sup>2</sup> Mark A. Reynolds, DDS, PhD,<sup>2</sup> Chongyun Bao, DDS, PhD,<sup>1</sup> Ping Wang, DDS, PhD,<sup>2</sup> Liang Zhao, MD, PhD,<sup>2,3</sup> and Hockin H.K. Xu, PhD<sup>2,4-6</sup>

A major challenge in repairing large bone defects with tissue-engineered constructs is the poor vascularization in the defect. The lack of vascular networks leads to insufficient oxygen and nutrients supply, which compromises the survival of seeded cells. To achieve favorable regenerative effects, prevascularization of tissue-engineered constructs by co-culturing of endothelial cells and bone cells is a promising strategy. The aim of this study was to investigate the effects of human-induced pluripotent stem cell-derived mesenchymal stem cells (hiPSC-MSCs) co-cultured with human umbilical vein endothelial cells (HUVECs) for prevascularization of calcium phosphate cement (CPC) scaffold on bone regeneration *in vivo* for the first time. HUVECs co-cultured with hiPSC-MSCs formed microcapillary-like structures *in vitro*. HUVECs promoted mineralization of hiPSC-MSCs on CPC scaffolds. Four groups were tested in a cranial bone defect model in nude rats: (1) CPC scaffold alone (CPC control); (2) HUVEC-seeded CPC (CPC-HUVEC); (3) hiPSC-MSC-seeded CPC (CPC-hiPSC-MSC); and (4) HUVECs co-cultured with hiPSC-MSCs on CPC scaffolds (co-culture group). After 12 weeks, the co-culture group achieved the greatest new bone area percentage of  $46.38\% \pm 3.8\%$  among all groups ( $p < 0.05$ ), which was more than four folds of the  $10.61\% \pm 1.43\%$  of CPC control. In conclusion, HUVECs co-cultured with hiPSC-MSCs substantially promoted bone regeneration. The novel construct of HUVECs co-cultured with hiPSC-MSCs delivered via CPC scaffolds is promising to enhance bone and vascular regeneration in orthopedic applications.

**Keywords:** endothelial cells, induced pluripotent stem cells, mesenchymal stem cells, vascularization, bone tissue engineering, animal model

## Introduction

IT IS STILL A GREAT CHALLENGE for orthopedic surgeons to reconstruct large skeletal defects. Traditional strategies often fail to repair large bone defects due to inadequate vascularization.<sup>1</sup> Tissue engineering methods are promising for bone reconstruction.<sup>2,3</sup> With scaffold delivery of cells, the cells inside the scaffold need sufficient nutrient and oxygen, usually diffusing from a nearby capillary network, for survival and normal function.<sup>1</sup> Cell viability in the scaffold is compromised if the distance from the nearest capillary network to the cells is greater than 100–200  $\mu\text{m}$ , which exceeds the diffusion or perfusion limit

of nutrients and oxygen.<sup>1</sup> Consequently, the regenerative capability of tissue-engineered constructs is greatly impeded with insufficient vascularization. Therefore, prevascularization is imperative for cell-based tissue-engineered bone constructs that are intended for large bone defect repair.<sup>4</sup> Prevascularization of the cell-seeded scaffold before implantation is expected to connect with host vasculature *in vivo* and supply the transplanted cells within the scaffold in a timely manner.<sup>4</sup>

Since endothelial cells (ECs) play a critical role in angiogenesis, many efforts have been made to achieve prevascularization of tissue-engineered products using ECs. It has been found that ECs are not only involved in the

<sup>1</sup>State Key Laboratory of Oral Diseases, West China Hospital of Stomatology, Sichuan University, Chengdu, Sichuan, China.

<sup>2</sup>Department of Endodontics, Periodontics and Prosthodontics, University of Maryland School of Dentistry, Baltimore, Maryland.

<sup>3</sup>Department of Orthopedic Surgery, Nanfang Hospital, Southern Medical University, Guangzhou, Guangdong, China.

<sup>4</sup>Center for Stem Cell Biology and Regenerative Medicine and <sup>5</sup>Marlene and Stewart Greenebaum Cancer Center, University of Maryland School of Medicine, Baltimore, Maryland.

<sup>6</sup>Mechanical Engineering Department, University of Maryland, Baltimore County, Maryland.

generation of new blood vessels<sup>5</sup> but also participate in the inflammatory response at an early implanted stage and in the subsequent repair process.<sup>6</sup> Specific pro-angiogenic factors that cannot be generated by ECs themselves are required for ECs to migrate and form microcapillaries.<sup>7</sup> Moreover, ECs alone can only form incipient vascular structures that resemble early capillaries.<sup>8</sup> These incipient vascular structures are unstable in the long term.<sup>8</sup>

For these reasons, in recent years, many studies examined co-culture systems of human osteogenic cells and ECs.<sup>9–11</sup> First, these co-culture systems promote the production of the essential pro-angiogenic factors that are generated by the cellular crosstalk between bone and ECs.<sup>7</sup> Second, vascular structures derived from these co-culture systems are stable.<sup>12</sup> Bone tissue engineering requires a complex architectural design composed of multiple cell types in combination with the scaffold to form a hierarchical organization for optimal bone restoration *in vivo*. Sources of osteogenic cells in co-culture with ECs include human osteoblast (OB) cell lines, primary OBs, and MSCs derived from a variety of tissue sources such as bone marrow, peripheral blood, adipose tissue, and various organs.<sup>7</sup>

Human-induced pluripotent stem cells (hiPSCs) are promising for bone tissue engineering. hiPSCs are generated from adult somatic cells with the reprogramming technique and these cells have advantageous characteristics of patient specificity, self-renewal capacity, functional similarities to embryonic stem cells, and less ethical controversy.<sup>13–15</sup> Interestingly, after hiPSCs are transduced to mesenchymal stem cells (hiPSC-MSCs), hiPSC-MSCs achieve great proliferation *in vitro* and their *in vivo* bone formation is comparable to that of traditional bone marrow-derived MSCs (BMSCs).<sup>15,16</sup> In addition, hiPSC-MSCs are less tumorigenic than hiPSCs.<sup>17,18</sup> For these reasons, we propose a novel system in which ECs and hiPSC-MSCs are co-cultured on a calcium phosphate cement (CPC) scaffold. This system takes advantage of interactions between ECs and hiPSC-MSCs to first promote prevascularization of CPC scaffolds *in vitro*, and then achieve bone regeneration *in vivo*. To our knowledge, this represents the first report on co-culturing hiPSC-MSCs with ECs on CPC scaffolds with bone regeneration *in vivo*.

Therefore, the objectives of this study were to: (1) investigate hiPSC-MSC co-cultured with human umbilical vein endothelial cells (HUVECs) for prevascularization of CPC scaffolds; (2) determine the osteogenic effects of HUVECs on hiPSC-MSCs *in vitro*; (3) and determine the *in vivo* osteogenic and angiogenic potential of the novel prevascularized tissue-engineered construct. It was hypothesized that: (1) hiPSC-MSCs co-cultured with HUVECs on macroporous CPC could form a prevascular network *in vitro*; (2) co-culturing with HUVECs could promote osteogenic differentiation of hiPSC-MSCs on CPC scaffolds; and (3) the prevascularized CPC scaffold would significantly enhance bone regeneration *in vivo*.

## Materials and Methods

### *Fabrication of macroporous CPC scaffolds*

CPC scaffold was prepared by following a previous study.<sup>19</sup> Briefly, TTCP [ $\text{Ca}_4(\text{PO}_4)_2\text{O}$ ] and DCPA ( $\text{CaHPO}_4$ ) powders at a 1:1 molar ratio were mixed to form the CPC powder. Rod-shaped, water-soluble mannitol crystals (Sig-

ma, St. Louis, MO) were used as a porogen to produce macropores in CPC. Mannitol particles that were around 125–250  $\mu\text{m}$  in size were mixed with CPC powder at a mannitol/(mannitol+CPC powder) mass fraction of 40%.<sup>20</sup> The CPC liquid contained 0.2 M  $\text{Na}_2\text{HPO}_4$  in distilled water to accelerate the setting reaction. A flowable CPC paste was prepared with the powder: liquid mass ratio of 2:1. The paste was placed in molds with a diameter of 5 mm and a thickness of 1 mm. After incubation in a humidifier for 1 day at 37°C, the disks were demolded and immersed in distilled water at 37°C for 3 days to dissolve the mannitol. The CPC scaffold had a macroporosity of  $50.9\% \pm 6.7\%$  and a total porosity of  $82.6\% \pm 2.4\%$  by volume.<sup>20</sup> The scaffold exhibited macropores from 100 to 300  $\mu\text{m}$  and micropores from 1 to 50  $\mu\text{m}$ .<sup>21</sup> The CPC scaffolds were sterilized in an ethylene oxide sterilizer (Andersen, Haw River, NC) for 12 h and then degassed for 7 days.

### *Cell culture and derivation of hiPSC-MSCs from hiPSCs*

The culture of hiPSCs was approved by the University of Maryland Baltimore Institutional Review Board (HP-00046649). Human hiPSC-Bc1 line was maintained on a mitotically inactivated murine embryonic fibroblasts (MEF) feeder.<sup>22</sup> The hiPSCs culture medium consisted of 80% Dulbecco's modified Eagle's medium (DMEM)/F12 (Invitrogen, Carlsbad, CA), 20% knockout serum replacement (a serum-free formulation; Invitrogen), 1% MEM non-essential amino acids solution, 10 ng/mL basic fibroblast growth factor (bFGF; Invitrogen), 1 mM L-glutamine (Sigma), and 0.1 mM  $\beta$ -mercaptoethanol (Sigma). hiPSCs were detached from MEF and dissociated into clumps by treatment with collagenase type IV. The dissociated hiPSC clumps were collected and induced to form embryoid bodies (EBs) in differentiation medium (the same formulation as hiPSC culture medium but without bFGF) in ultra-low attachment cell culture flasks (Corning, Corning, NY). The EBs were transferred onto 0.1% gelatin-coated culture dishes after 10 days of suspension culture. Cells gradually migrated out from EBs and were selectively isolated by using cell scrapers.

The selected cells (P0) were sub-cultured in MSC growth medium, which consisted of low-glucose DMEM (Gibco, Grand Island, NY) that was supplemented with 10% fetal bovine serum (FBS; HyClone, Logan, UT), 100 U/mL penicillin, and 100 mg/mL streptomycin (PS; Gibco). It was confirmed by our previous study that more than 90% of the hiPSC-MSCs expressed MSC surface markers (CD29, CD44, CD166, CD73), and they were negative for typical hematopoietic (CD34), endothelial (CD31), and pluripotent markers (TRA-1-81 and OCT 3/4).<sup>22</sup> The hiPSC-MSCs could differentiate into three characteristic mesenchymal lineages, including OBs, adipocytes, and chondrocytes.<sup>23</sup> Passage 3–5 hiPSC-MSCs were used for the following experiments.

HUVECs (Lonza, Walkersville, MD) were cultured in endothelial cell growth medium-2 (EGM-2; Lonza). The fourth-passage HUVECs were used.

### *Cell seeding on macroporous CPC scaffolds*

Three cell-seeded groups were investigated. (1) hiPSC-MSCs-seeded CPC. hiPSC-MSCs were seeded on CPC at

$1.5 \times 10^5$  cells/scaffold and cultured in MSC growth medium. (2) HUVECs-seeded CPC. HUVECs were seeded on CPC at  $1.5 \times 10^5$  cells/scaffold and cultured in EGM-2. (3) Co-culture of hiPSC-MSCs with HUVECs. HUVECs were mixed with hiPSC-MSCs at a 3:1 ratio, seeded on CPC at  $1.5 \times 10^5$  cells/scaffold, and cultured in EGM-2.<sup>24</sup> The medium was replaced every 2 days.

#### Cell attachment and viability

Live/dead staining (Molecular Probes, Eugene, OR) was used to test cell viability of co-cultured HUVECs and hiPSC-MSCs on macroporous CPC at 4, 7, 14, and 21 days. Cell co-seeded disks were washed with PBS and incubated with  $4 \mu\text{M}$  ethidium homodimer-1 and  $2 \mu\text{M}$  calcein-AM in PBS for 20 min. The disks were then examined by using epifluorescence microscopy (Eclipse TE2000-S; Nikon, Melville, NY). The percentage of live cells ( $P$ ) and the live cell density ( $D$ ) were calculated as previously described.<sup>16</sup>  $P = \text{number of live cells} / (\text{number of live cells} + \text{number of dead cells})$ .  $D = \text{number of live cells in the image} / \text{the image area}$  ( $n = 5$ ).

#### Immunofluorescent staining of PECAM-1 (CD31)

An endothelial-specific anti-PECAM-1 (CD31) (Invitrogen) antibody was used to identify microvascular structure on CPCs at 7, 14, and 21 days.<sup>19,25</sup> The samples were fixed with 4% paraformaldehyde for 20 min, then permeabilized with 0.5% Triton X-100 for 5 min, and finally blocked with 0.1% bovine serum albumin for 30 min. The samples were incubated with the primary mouse monoclonal anti-human CD31 antibody (1:200; Invitrogen) at  $4^\circ\text{C}$  overnight, followed by room temperature incubation with secondary antibody goat anti-mouse Alexa Fluor 488 (green fluorescence) (Invitrogen) for 1 h. DAPI ( $1 \mu\text{g}/\text{mL}$ ; Sigma) was used to stain cell nuclei. The microvascular structures were shown as green tube-like structures. The HUVECs-seeded CPC scaffold was used as the control.

#### Scanning electron microscopy of cells on CPC

At 21 days, the cell-seeded scaffolds were fixed with 2% glutaraldehyde, dehydrated with gradient ethanol, sputter-coated with gold, and examined under scanning electron microscopy (SEM, Quanta 200; FEI, Hillsboro, OR).

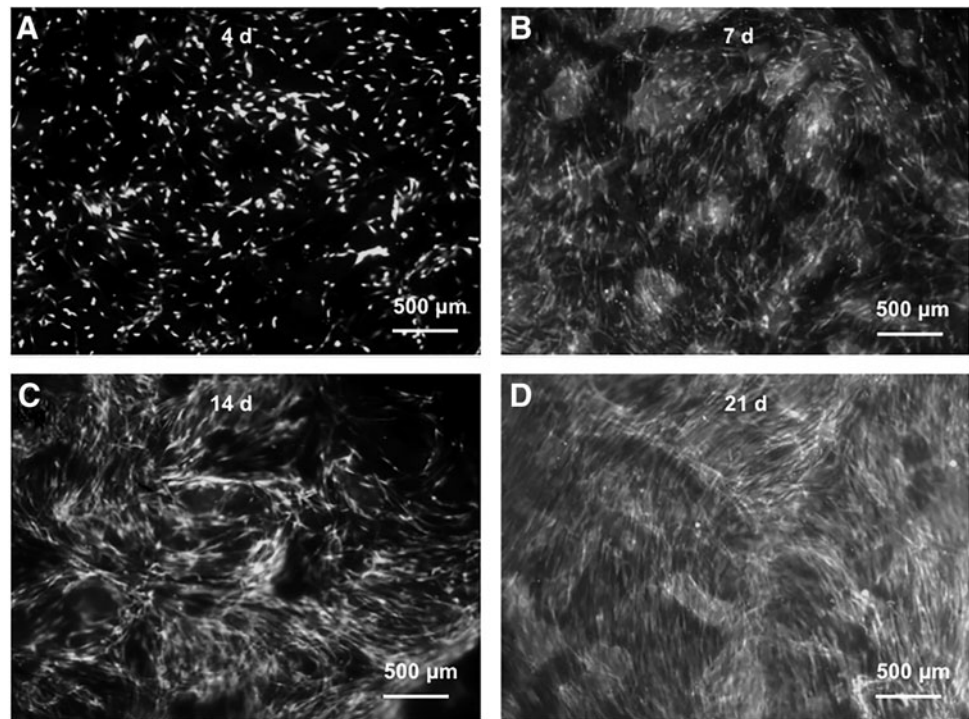
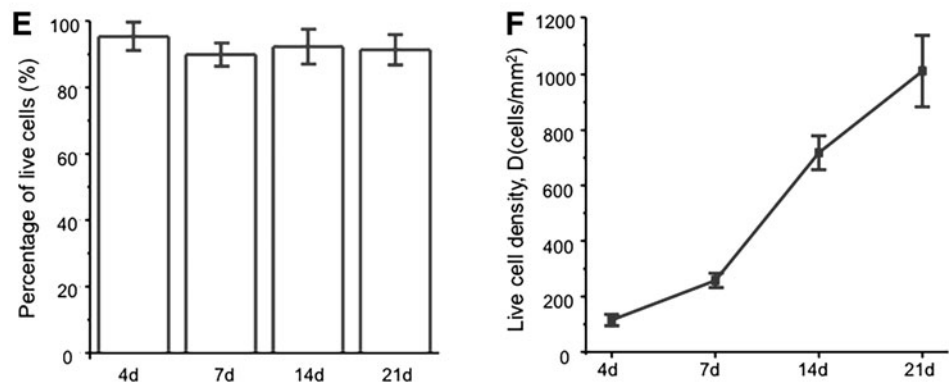


**FIG. 1.** Live/dead assay of HUVECs and iPSC-MSCs co-cultured on CPC scaffolds. The images at 4, 7, 14, and 21 days are shown in (A–D). (E) The percentage of live cells. (F) The density of live cells ( $n = 5$ ). CPC, calcium phosphate cement; HUVECs, human umbilical vein endothelial cells; iPSC-MSCs, induced pluripotent stem cell-derived mesenchymal stem cells.



### Mineralization assays

The osteogenetic ability of cell-seeded scaffolds was detected by alizarin red S (ARS) staining of calcium-rich deposits at 7, 14, and 21 days. The samples were fixed with 10% formaldehyde and stained with ARS (Millipore, Billerica, MA) for 20 min. Then, the disks were rinsed with deionized water and the presence of calcified deposition of cells on scaffolds was visualized.<sup>16</sup> An Osteogenesis Quantitation Kit (Millipore; ECM 815) was used to extract the stained minerals and to measure the ARS concentration, following the manufacturer's instructions ( $n=5$ ). The ARS standard curve was constructed with known concentrations of the dye.<sup>26</sup> CPC disks without cells served as the control, and with the same treatments and measured in the same manner. The control's ARS concentration was subtracted from the ARS concentration of disks with cells to yield the net mineral concentration synthesized by cells, by following the method reported in a previous study.<sup>26</sup>

### In vivo cranial bone defects in rats

Two symmetric full-thickness cranial defects of 5 mm diameter were created on the parietal bone of 12 male athymic nude rats, with one defect on each side of the sagittal suture (Hsd:RH-Fox1<sup>tmu</sup>, 200–250 g, 8 week-old; Harlan, Indianapolis, IN) by following a protocol approved by the University of Maryland Baltimore (IACUC No.

0909014) and NIH animal-care guidelines. This model has been used in previous studies.<sup>27,28</sup> Briefly, under general anesthesia, two full-thickness 5 mm defects were made in the calvarium under continuous saline irrigation.<sup>27</sup> Four groups were tested: (1) CPC scaffold only (CPC control); (2) hiPSC-MSCs-seeded CPC group (CPC-hiPSC-MSCs); (3) HUVECs-seeded CPC group (CPC-HUVECs); and (4) hiPSC-MSCs and HUVECs-seeded CPC group (co-culture). Cells were seeded and cultured on CPC scaffolds for 21 days before *in vivo* implantation. The rats were sacrificed, and the grafts were harvested after 12 weeks ( $n=6$ ).

### Histomorphometry analyses

Specimens were decalcified and embedded in paraffin. The central part of the implant and defect was cut into 5  $\mu\text{m}$ -thick sections and stained with hematoxylin and eosin (HE). One slide per construct was selected for the analysis. New bone area and total defect area were measured within the boundaries of defects in each section by Image Pro Plus Software (Media Cybernetics, Carlsbad, CA). The perimeter around the new bone was traced, and the area of the new bone was measured by the software. New bone area percentage was calculated as the new bone area divided by the total defect area ( $n=6$ ).<sup>26</sup> Blood vessels were identified by their luminal structure and the presence of red blood cells within their

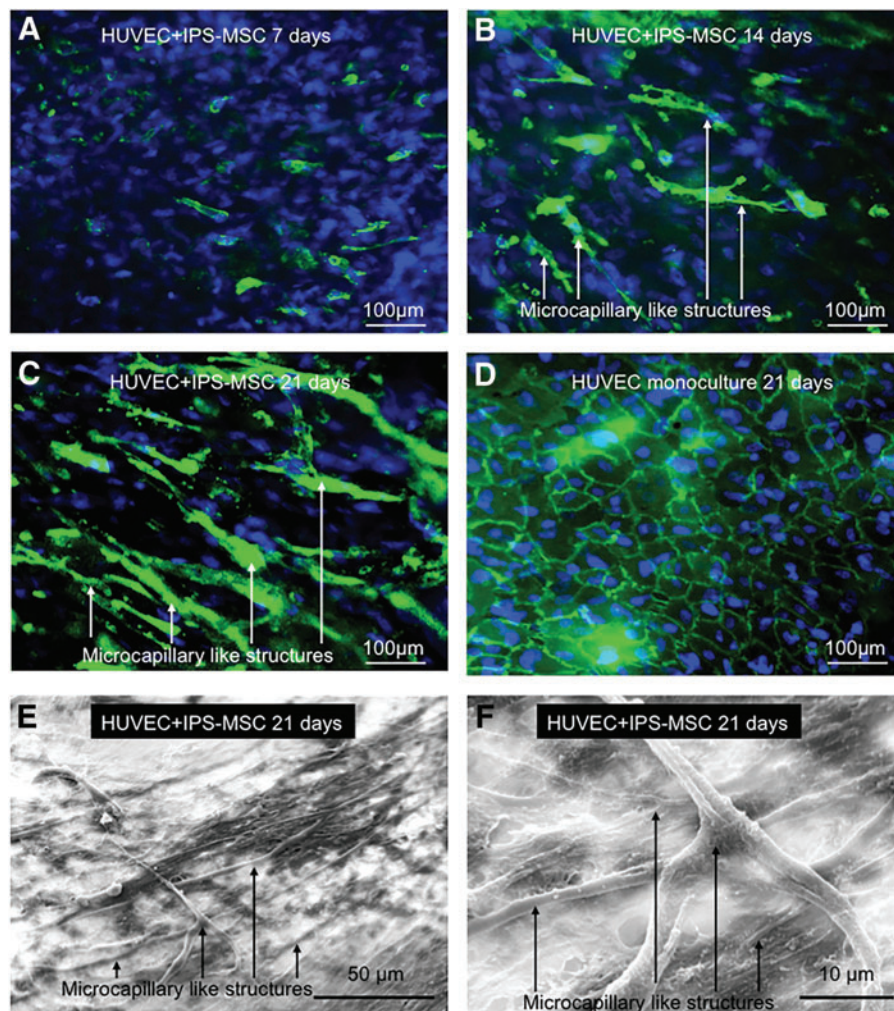


**FIG. 2.** The formation of microcapillary like structures formed by HUVECs and iPSC-MSCs co-cultured on CPC scaffolds (A–C). HUVECs were identified by immunostaining with endothelial marker PECAM-1 in green on the cell membrane, and the nuclei were stained with DAPI in blue. iPSC-MSCs were depicted by nuclei counterstaining with DAPI in blue but without green stains on the cell membrane. Microcapillary-like structures increased with culture time. (D) The HUVEC monoculture control group, which had no vascular-like structures observed. Representative scanning electron microscopy images of microcapillary-like structures formed by the co-culture system (E, F). These images show examples of microcapillary structures on CPC at 21 days. Image F is a higher magnification of image (E). Color images available online at [www.liebertpub.com/tea](http://www.liebertpub.com/tea)



boundaries at the magnification of  $\times 200$ . The blood vessel density was calculated by the number of blood vessels in the defect area divided by the entire defect area ( $n=6$ ).<sup>27</sup>

### Statistical analyses

Statistical Package for the Social Sciences (SPSS 17.0, Chicago, IL) was used for statistical analyses. All data were expressed as the mean value  $\pm$  standard deviation. The Levene test was first performed to confirm that the normality and equal variance assumptions of the data were not violated. Statistical significance was assessed by using one-way analysis of variance followed by *post hoc* least-significant difference tests. A probability value ( $p$ ) of less than 0.05 was considered statistically significant.

### Results

The representative images of live/dead staining of HUVECs and hiPSC-MSCs co-cultured on CPC scaffolds at 4, 7, 14, and 21 days are shown in Figure 1A–D. There were numerous live cells (green staining) and a few dead cells (red staining) at each time point. The percentages of live cells on CPC scaffolds were more than 90% at each time point (Fig. 1E). The number of live cells increased with time (Fig. 1F). The density of live cells increased by about 8-fold from 4 to 21 days.

Figure 2A–C showed the PECAM-1 immunofluorescent staining images of HUVECs and hiPSC-MSCs that were co-cultured on macroporous CPC scaffolds. HUVECs were identified by the green staining of endothelial marker PECAM-1 on the cell membrane. At 7 days, HUVECs were arranged at several bud points (Fig. 2A). The bud points gradually grew longer and formed microcapillary-like structures at 14 and 21 days (Fig. 2B). At 21 days, the self-assembling organization of microcapillary-like structures on CPC scaffolds became more complex and interwoven with each other (Fig. 2C). This result was in accordance with the SEM images of co-cultured cells on CPC scaffolds at 21 days (Fig. 2E, F). At 21 days, the CPC scaffolds were completely covered by cells, and numerous microcapillary-like structures formed on the surface of cell layers. At high magnification, it was observed that the microcapillary-like structures formed a meshwork (Fig. 2F). In contrast, there was no such organized tube-like structure in the HUVECs-seeded CPC group at 21 days; instead, cells exhibited a confluent flat cell layer (Fig. 2D).

Figure 3A showed ARS staining of cell-synthesized matrix on macroporous CPC scaffolds at 7 and 21 days. Compared with the hiPSC-MSCs monoculture group, the co-culture group exhibited a denser and darker red color and more granular-like bone nodules deposited at 21 days. From 7 to 21 days, there was a significant increase of mineral concentration in the co-culture group (Fig. 3B). These results indicated that co-seeding of HUVECs and hiPSC-MSCs on CPC could promote osteogenic differentiation and mineralization of hiPSC-MSCs on CPC scaffolds.

The representative H&E histological images at 12 weeks were shown in Figure 4A–D. The cell-seeded groups (Fig. 4A–C) exhibited markedly more new bone (indicated by the arrows) in the defect area than the CPC control group (Fig. 4D). In all groups, extracellular matrix and new bone deposition were mainly found at the peripherals of the CPC scaffolds, where more sufficient nutrient and oxygen diffused from native circumstances. The co-culture group showed the

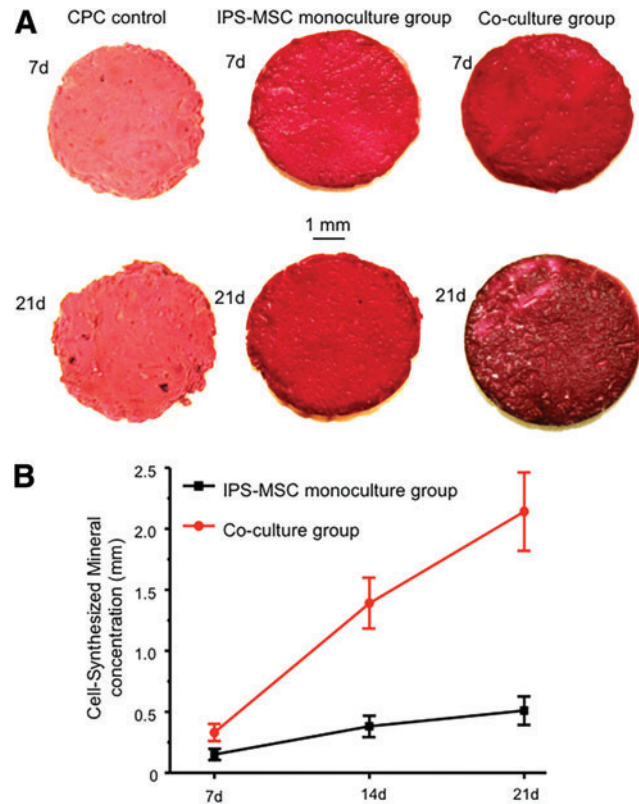


**FIG. 3.** The mineral synthesis by cells on CPC scaffolds. Alizarin red S staining showed that the co-culture group exhibited a denser and thicker layer of red-stained bone nodules than the mono-culture group and the CPC control group (A). (B) The quantitative osteogenesis assay, which indicated greater mineral synthesis by the co-culture group than the monoculture group ( $n=5$ ). Color images available online at [www.liebertpub.com/tea](http://www.liebertpub.com/tea)

highest amount of new bone deposited in and around the CPC scaffolds among the four groups (Fig. 4A), whereas the CPC control group showed the least new bone formation (Fig. 4D).

High magnification images are shown in Figure 5. Figure 5A was from the co-culture group (the dotted area in Fig. 4A). At 12 weeks, the newly formed bone inside the scaffold area exhibited typical mature bone morphology. Calcified bone matrix presented as a deep red dense matrix, with some osteocytes embedded inside. Figure 5B is taken from the CPC-HUVECs group (the dotted area in Fig. 4C). New blood vessels were formed inside of the defect area and surrounded by some loose connective tissue. The new blood vessels contain a rich supply of erythrocytes inside the tube-like structure lined by a layer of ECs.

The new bone area fraction in the co-culture group was  $46.38\% \pm 3.8\%$ , which was significantly higher than the other three groups ( $p < 0.05$ ). The CPC-hiPSC-MSCs group had more new bone than the CPC-HUVECs group ( $p < 0.05$ ), whereas the CPC control group exhibited the least new bone formation at  $10.61\% \pm 1.43\%$ . Figure 6B showed the new blood vessel density. The CPC-HUVECs group had the most new blood vessel density than the other three groups. And the CPC control group had the least number of blood vessels ( $p < 0.05$ ). The co-culture group had more new blood vessel density than CPC-hiPSC-MSCs and the CPC control group ( $p < 0.05$ ).

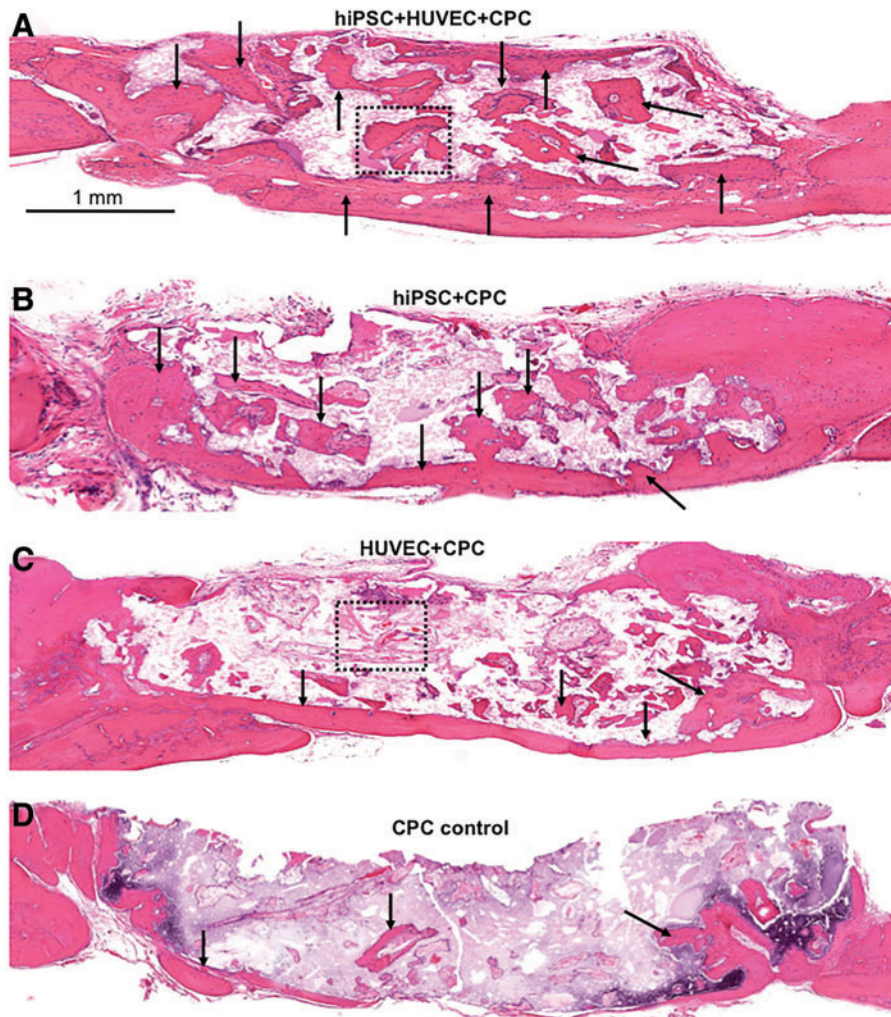


**FIG. 4.** The representative H&E staining histological images after 12-week implantation *in vivo*. Mineralized new bone was stained in red (as dark arrow show), whereas white area was due to slight detachment of the tissue or decalcification of residual CPC. The dura side is on the bottom of the image. The cell-seeded groups showed more new bone than the CPC control group. A markedly amount of new bone formation was observed in the co-culture group. (A–D) Are representative H&E images from different groups: (A) hiPSC+HUVEC+CPC; (B) hiPSC+CPC; (C) HUVEC+CPC; (D) CPC control. Color images available online at [www.liebertpub.com/tea](http://www.liebertpub.com/tea)

## Discussion

In this study, we presented evidence that the co-culturing of hiPSC-MSCs and HUVECs on CPC scaffolds enhanced the formation of capillary-like structures before *in vivo* implantation. Co-cultured HUVECs also promoted bone formation by hiPSC-MSCs. When the prevascularized scaffold was implanted *in vivo*, a significant amount of new bone formation was observed in the co-culture group.

The use of hiPSC-MSCs has shown promising results in bone tissue engineering. It has been reported that telomerase activity is 10-fold greater in hiPSC-MSCs than in BMSCs and hiPSC-MSCs are capable of doubling as many as 120 populations without obvious loss of plasticity or the onset of replicative senescence.<sup>15</sup> With this robust cell viability and self-renewal capability, superior survival and engraftment can be expected after transplantation of hiPSC-MSCs.<sup>15</sup> hiPSC-MSCs can be successfully differentiated down the osteogenic cell lineage, as demonstrated by enhanced alkaline phosphatase (ALP) activity, upregulated osteogenic-related genes, and increased mineral deposition *in vitro*.<sup>22,23,29–35</sup> Several recent *in vivo* studies present important evidence to show *de novo* bone formation or mineral deposition in hiPSC-MSC-implanted scaffolds and direct involvement of transplanted hiPSC-MSCs in bone regeneration.<sup>16,31–33</sup> In the present study, CPC-hiPSC-MSCs groups exhibited

$34.4\% \pm 3.0\%$  of new bone area percentage, which is, in general, comparable to previous reports of new bone area percentage at  $22.5\% \pm 7.6\%$  to  $30.4\% \pm 5.8\%$  in hiPSC-MSC-seeded groups.<sup>18,27</sup> The difference in the values could be attributed to different animal models and different material constructs. To further boost its bone regenerative potential, in this study, we introduce the concept of HUVECs-mediated vascularization to the hiPSC-MSC-based bone tissue engineering, because prevascularization can advance the performance of transplanted cells in tissue-engineered scaffolds<sup>12</sup> and a vascular network must be established that precedes osteogenesis and, thus, would lead to the formation of a metabolically active bone graft.<sup>12</sup> To this end, we tested the *in vitro* and *in vivo* angiogenic and osteogenic performance of HUVECs and hiPSC-MSCs co-cultured on CPC scaffolds.

In the present study, single-cell cultures of HUVECs on CPC scaffolds failed to self-assemble to form microcapillary-like structures. In contrast, sprouting microcapillary-like structures were observed in the co-culture model of HUVECs and hiPSC-MSCs. In addition, a synergistic effect between angiogenesis and osteogenesis was also observed in the present study. Co-culture systems of HUVECs and hiPSC-MSCs were found to promote mineralization even in the absence of any osteogenic supplements. The cellular crosstalk between vessel-forming cells, such as ECs, and bone-forming cells, such as OBs (derived from either primary cultured cells or progenitors,

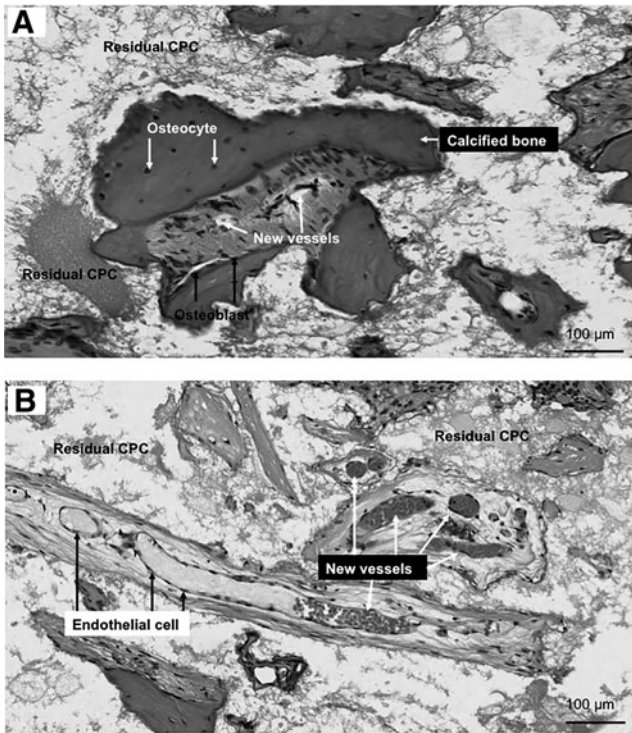


**FIG. 5.** High magnification images of new bone extracted from dotted rectangles in the co-culture group (A) and the CPC-HUVEC group (B). The co-culture group exhibited more calcified new bone within the defects than the monoculture group. New blood vessels were found in the macropores of CPC scaffolds.

such as MSCs), has been well documented.<sup>36–54</sup> With regard to the effects of angiogenesis, it has been reported that OBs or OBs derived from MSCs can secrete numerous proangiogenic factors, including VEGF,<sup>37–44</sup> Ang-1, -2,<sup>43,45</sup> VE-cadherin,<sup>17</sup> IGF-1,<sup>46</sup> IGF-2,<sup>44</sup> PDGFB/PDBFR $\beta$ ,<sup>44</sup> bFGF,<sup>47</sup> and so on, to influence EC activity. Notably, VEGF is the most frequently identified factor that is upregulated in the co-culture system,

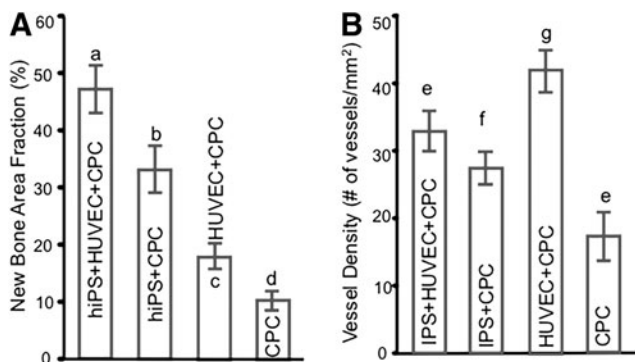


**FIG. 6.** The histomorphometric analysis of new bone area fraction (A) and new blood vessel density (B). The co-culture group showed the highest amount of new bone formation than the other three groups ( $p < 0.05$ ). The CPC control group had the least amount of new bone formation and blood vessels number in all groups ( $p < 0.05$ ). Each value is mean  $\pm$  standard deviation ( $n = 6$ ). Dissimilar letters indicated significantly different values ( $p < 0.05$ ).

which contributes to the neovascularization.<sup>37–44</sup> Moreover, MSCs may act as perivascular cells to stabilize and maintain vascular structures.<sup>48–50</sup> On the other hand, ECs not only augment cell proliferation of bone-forming cells<sup>51,52</sup> but also release numerous regulatory molecules, such as ALP,<sup>40,53–55</sup> osteocalcin,<sup>25</sup> runt-related transcription factor 2 (Runx2),<sup>25</sup> and BMP-2,<sup>56</sup> to control the differentiation and activity of the co-cultured bone-forming cells. Among these factors, ALP is often the factor that is mentioned as stimulated to promote early commitment of the cells down to the osteogenic lineage.<sup>40,53–55</sup> Its secretion has been shown to be dependent on the direct contact of ECs with OBs with the involvement of connexin43 as the gap junction to increase ALP expression in the co-cultures.<sup>52</sup> Mineralization, an endpoint of osteogenic differentiation, is also enhanced in the co-culture system.<sup>19,25</sup> It is consistent with the finding of the current study that the co-culture group exhibited more bone nodule deposits than the monoculture group. Such cell–cell communication has been reported between ECs and various MSCs, such as umbilical vein MSCs,<sup>57</sup> adipose-derived MSCs,<sup>58–60</sup> human dental pulp stem cells,<sup>60</sup> and BMSCs.<sup>48,58,61</sup> To the best of our knowledge, there has been no report of the co-culture of hiPSC-MSCs and ECs. Our *in vitro* results indicated that the co-culture of hiPSC-MSCs and ECs had a synergistic effect of vascularization and mineralization on the CPC scaffold. One factor that should be considered regarding the difference between the mono-cultured hiPSC-MSC group and the co-culture group is that an MSC growth medium was used for the hiPSC-MSC group, whereas an EGM-2 was used for the co-culture group. It is possible that, in addition to the influence of the co-cultured HUVECs on the hiPSC-MSCs, the multiple angiogenic growth factors in EGM-2 also affected the biology of hiPSC-MSCs and their behavior in the co-culture group. The present study was designed to compare different strategies for potential clinical applications, namely monoculture cell strategy versus co-culture cell strategy. From the perspective of application, EGM-2 is not a regular culture medium for hiPSC-MSCs. Therefore, we used MSC growth medium for the hiPSC-MSC monoculture group.

Our study represented the first report on the co-culture system of hiPSC-MSCs and ECs to prevascularize CPC scaffolds targeting bone regeneration. Our *in vivo* study showed that the co-culture group exhibited a significantly higher amount of new bone deposition than the monoculture groups and the CPC control group at 3 months, even though the highest blood vessel density was found in the CPC-HUVEC group and not in the co-culture group. It was attributed to the fact that at 3 months, the bone remodeling process had already taken place. In calvaria where compact bone presents as the major part, the more mature the bone is, the less spaces or hollows in the bone matrix are. Thus, there were fewer blood vessels in the co-culture group than in the CPC-HUVEC group at 3 months in a corticalization process of the calvarial bone defect. It was possible that at early time points, the co-culture group established higher vascular supply than the other groups, which promoted subsequent bone formation, maturing, and integration of live and functional bone grafts. Interestingly, there are many recent efforts engaged in deriving ECs from hiPSCs (iPSC-ECs). The generated hiPSC-ECs show an EC-specific phenotype and cell morphology and they are capable of forming microcapillary like structures *in vitro* and neovascularization



*in vivo* after implantation.<sup>62,63</sup> hiPSC-ECs with a nearly unlimited passage potential may become an alternative source for HUVECs. It is our next step to investigate the co-culture of hiPSC-MSCs and hiPSC-ECs targeting vascularization and bone regeneration. The current study provides preliminary evidence to show the synergistic effects of ECs and hiPSC-MSCs. The utilization of hiPSC-derived cells to achieve vessel and bone formation in bone tissue engineering is a promising strategy.

Finally, this study was limited in several ways. First, we did not perform specific staining and immunohistological staining to specifically identify new bone and blood vessels. The new bone and new blood vessel identification and assessment in this study was based on morphological characteristics of tissues via HE staining. It is possible that some delicate structures such as nascent micro-vessels were not adequately detected and, thus, not included in the evaluation. Second, we did not perform additional tests other than histological tests for the *in vivo* study. Future study should evaluate gene and/or protein expressions, 3D imaging of the vascularization, and micro-CT measurements. Third, even though the 5 mm calvarial bone defect model in rats was previously considered a critical-sized defect,<sup>28</sup> according to the latest authoritative protocol,<sup>64</sup> an 8 mm-diameter defect is generally accepted to be the critical size in the rat calvarial bone. Thus, the data should be explained with consideration of contribution of the natural regenerative capacity. Fourth, this study only investigated the co-culture prevascularization strategy. Other prevascularization methods, such as the two-step *in vivo* prevascularization strategy involving the initial implantation of tissue-engineered grafts in rich vascularized sites for complete vascularization before subsequent implantation at the defect site, are not compared in the current study. Future study is needed to compare the reperfusion efficacy of various *in vivo* and *in vitro* prevascularization strategies.

In conclusion, our study is the first study to investigate the prevascularization strategy of co-culturing hiPSC-MSCs and ECs on CPC scaffolds. An *in vitro* study showed that the co-culture system enhanced the formation of capillary-like structures and co-cultured ECs promoted osteogenesis and mineralization of hiPSC-MSCs. When the prevascularized scaffold was implanted *in vivo*, a significant amount of new bone formation was observed in the co-culture group. These findings not only elucidate an intimate connection between angiogenesis and osteogenesis but also provide important evidences in advancing the emerging field of hiPSC-MSC-driven bone tissue regeneration.

#### Acknowledgments

The authors thank Dr. Linzhao Cheng for generously providing the hiPSC BC1 cell line. This study was supported by the National Science Foundation of China 31400829 (X.L.) and 81401794 (P.W.), the Sichuan Provincial Science and Technology Department Foundation of China 2014JY0076 (X.L.), the National Key Research and Development Program of China 2016YFC1102700 (C.B.), and the University of Maryland School of Dentistry.

#### Disclosure Statement

No competing financial interests exist.

#### References

1. Lovett, M., Lee, K., Edwards, A., and Kaplan, D.L. Vascularization strategies for tissue engineering. *Tissue Eng Part B Rev* **15**, 353, 2009.
2. Salgado, A.J., Coutinho, O.P., and Reis, R.L. Bone tissue engineering: state of the art and future trends. *Macromol Biosci* **4**, 743, 2004.
3. Service, R.F. Tissue engineers build new bone. *Science* **289**, 1498, 2000.
4. Liu, Y., Chan, J.K., and Teoh, S.H. Review of vascularised bone tissue-engineering strategies with a focus on co-culture systems. *J Tissue Eng Regen Med* **9**, 85, 2015.
5. Hirschi, K.K., Skalak, T.C., Peirce, S.M., and Little, C.D. Vascular assembly in natural and engineered tissues. *Ann N Y Acad Sci* **961**, 223, 2002.
6. Peters, K., Unger, R.E., Brunner, J., and Kirkpatrick, C.J. Molecular basis of endothelial dysfunction in sepsis. *Cardiovasc Res* **60**, 49, 2003.
7. Unger, R.E., Dohle, E., and Kirkpatrick, C.J. Improving vascularization of engineered bone through the generation of pro-angiogenic effects in co-culture systems. *Adv Drug Deliv Rev* **94**, 116, 2015.
8. Koike, N., Fukumura, D., Gralla, O., Au, P., Schechner, J.S., and Jain, R.K. Tissue engineering: creation of long-lasting blood vessels. *Nature* **428**, 138, 2004.
9. Rouwkema, J., Boer, J.D., and Blitterswijk, C.A.V. Endothelial cells assemble into a 3-dimensional prevascular network in a bone tissue engineering construct. *Tissue Eng* **12**, 2685, 2006.
10. Unger, R.E., Sartoris, A., Peters, K., Motta, A., Migliaresi, C., Kunkel, M., Bulnheim, U., Rychly, J., and Kirkpatrick, C.J. Tissue-like self-assembly in cocultures of endothelial cells and osteoblasts and the formation of microcapillary-like structures on three-dimensional porous biomaterials. *Biomaterials* **28**, 3965, 2007.
11. Santos, M.I., Unger, R.E., Sousa, R.A., Reis, R.L., and Kirkpatrick, C.J. Crosstalk between osteoblasts and endothelial cells co-cultured on a polycaprolactone–starch scaffold and the *in vitro* development of vascularization. *Biomaterials* **30**, 4407, 2009.
12. Brennan, M.A., Davaine, J.-M., and Layrolle, P. Prevascularization of bone tissue-engineered constructs. *Stem Cell Res Ther* **4**, 1, 2013.
13. Takahashi, K., Tanabe, K., Ohnuki, M., Narita, M., Ichisaka, T., Tomoda, K., and Yamanaka, S. Induction of pluripotent stem cells from adult human fibroblasts by defined factors. *Cell* **131**, 861, 2007.
14. Robinton, D.A., and Daley, G.Q. The promise of induced pluripotent stem cells in research and therapy. *Nature* **481**, 295, 2012.
15. Lian, Q., Zhang, Y., Zhang, J., Zhang, H.K., Wu, X., Zhang, Y., Lam, F.F.-Y., Kang, S., Xia, J.C., and Lai, W.-H. Functional mesenchymal stem cells derived from human induced pluripotent stem cells attenuate limb ischemia in mice. *Circulation* **121**, 1113, 2010.
16. Wang, P., Liu, X., Zhao, L., Weir, M.D., Sun, J., Chen, W., Man, Y., and Xu, H.H. Bone tissue engineering via human induced pluripotent, umbilical cord and bone marrow mesenchymal stem cells in rat cranium. *Acta Biomater* **18**, 236, 2015.
17. Zhao, Q., Gregory, C.A., Lee, R.H., Reger, R.L., Qin, L., Hai, B., Park, M.S., Yoon, N., Clough, B., and McNeill, E. MSCs derived from iPSCs with a modified protocol are tumor-tropic but have much less potential to promote tu-



- mors than bone marrow MSCs. *Proc Natl Acad Sci U S A* **112**, 530, 2015.
18. Wei, H., Tan, G., Qiu, S., Kong, G., Yong, P., Koh, C., Ooi, T.H., Lim, S.Y., Wong, P., and Gan, S.U. One-step derivation of cardiomyocytes and mesenchymal stem cells from human pluripotent stem cells. *Stem Cell Res* **9**, 87, 2012.
  19. Chen, W., Thein-Han, W., Weir, M.D., Chen, Q., and Xu, H.H. Prevascularization of biofunctional calcium phosphate cement for dental and craniofacial repairs. *Dent Mater* **30**, 535, 2014.
  20. Xu, H.H., Weir, M.D., Burguera, E.F., and Fraser, A.M. Injectable and macroporous calcium phosphate cement scaffold. *Biomaterials* **27**, 4279, 2006.
  21. Liu, X., Wang, P., Chen, W., Weir, M.D., Bao, C., and Xu, H.H.K. Human embryonic stem cells and macroporous calcium phosphate construct for bone regeneration in cranial defects in rats. *Acta Biomater* **10**, 4484, 2014.
  22. Liu, J., Chen, W., Zhao, Z., and Xu, H.H. Reprogramming of mesenchymal stem cells derived from iPSCs seeded on biofunctionalized calcium phosphate scaffold for bone engineering. *Biomaterials* **34**, 7862, 2013.
  23. Tang, M., Chen, W., Liu, J., Weir, M.D., Cheng, L., and Xu, H.H. Human induced pluripotent stem cell-derived mesenchymal stem cell seeding on calcium phosphate scaffold for bone regeneration. *Tissue Eng Part A* **20**, 1295, 2014.
  24. Bidarra, S.J., Barrias, C.C., Barbosa, M.A., Soares, R., Amédée, J., and Granja, P.L. Phenotypic and proliferative modulation of human mesenchymal stem cells via crosstalk with endothelial cells. *Stem Cell Res* **7**, 186, 2011.
  25. Thein-Han, W., and Xu, H.H. Prevascularization of a gas-foaming macroporous calcium phosphate cement scaffold via coculture of human umbilical vein endothelial cells and osteoblasts. *Tissue Eng Part A* **19**, 1675, 2013.
  26. Chen, W., Liu, J., Manuchehrabadi, N., Weir, M.D., Zhu, Z., and Xu, H.H. Umbilical cord and bone marrow mesenchymal stem cell seeding on macroporous calcium phosphate for bone regeneration in rat cranial defects. *Biomaterials* **34**, 9917, 2013.
  27. Wang, P., Song, Y., Weir, M.D., Sun, J., Zhao, L., Simon, C.G., and Xu, H.H. A self-setting iPSCMSC-alginate-calcium phosphate paste for bone tissue engineering. *Dent Mater* **32**, 252, 2016.
  28. Zou, D., Zhang, Z., He, J., Zhu, S., Wang, S., Zhang, W., Zhou, J., Xu, Y., Huang, Y., Wang, Y., Han, W., Zhou, Y., Wang, S., You, S., Jiang, X., and Huang, Y. Repairing critical-sized calvarial defects with bmscs modified by a constitutively active form of hypoxia-inducible factor-1 $\alpha$  and a phosphate cement scaffold. *Biomaterials*, **32**, 9707, 2011.
  29. Chen, Y.S., Pelekanos, R.A., Ellis, R.L., Horne, R., Wolvetang, E.J., and Fisk, N.M. Small molecule mesengenic induction of human induced pluripotent stem cells to generate mesenchymal stem/stromal cells. *Stem Cells Transl Med* **1**, 83, 2012.
  30. Liu, Y., Goldberg, A.J., Dennis, J.E., Gronowicz, G.A., and Kuhn, L.T. One-step derivation of mesenchymal stem cell (MSC)-like cells from human pluripotent stem cells on a fibrillar collagen coating. *PLoS One* **7**, e33225, 2012.
  31. Villa-Diaz, L., Brown, S., Liu, Y., Ross, A., Lahann, J., Parent, J., and Krebsbach, P. Derivation of mesenchymal stem cells from human induced pluripotent stem cells cultured on synthetic substrates. *Stem Cells* **30**, 1174, 2012.
  32. Zou, L., Luo, Y., Chen, M., Wang, G., Ding, M., Petersen, C.C., Kang, R., Dagnaes-Hansen, F., Zeng, Y., and Lv, N. A simple method for deriving functional MSCs and applied for osteogenesis in 3D scaffolds. *Sci Rep* **3**, 2243, 2013.
  33. Hynes, K., Menicanin, D., Han, J., Marino, V., Mrozik, K., Gronthos, S., and Bartold, P. Mesenchymal stem cells from iPSC cells facilitate periodontal regeneration. *J Dent Res* **92**, 833, 2013.
  34. Diederichs, S., and Tuan, R.S. Functional comparison of human-induced pluripotent stem cell-derived mesenchymal cells and bone marrow-derived mesenchymal stromal cells from the same donor. *Stem Cells Dev* **23**, 1594, 2014.
  35. Hynes, K., Menicanin, D., Mrozik, K., Gronthos, S., and Bartold, P.M. Generation of functional mesenchymal stem cells from different induced pluripotent stem cell lines. *Stem Cells Dev* **23**, 1084, 2013.
  36. Grellier, M., Bordenave, L., and Amedee, J. Cell-to-cell communication between osteogenic and endothelial lineages: implications for tissue engineering. *Trends Biotechnol* **27**, 562, 2009.
  37. Fu, W.-L., Xiang, Z., Huang, F.-G., Gu, Z.-P., Yu, X.-X., Cen, S.-Q., Zhong, G., Duan, X., and Liu, M. Coculture of peripheral blood-derived mesenchymal stem cells and endothelial progenitor cells on strontium-doped calcium polyphosphate scaffolds to generate vascularized engineered bone. *Tissue Eng Part A* **21**, 948, 2014.
  38. Kolbe, M., Xiang, Z., Dohle, E., Tonak, M., Kirkpatrick, C.J., and Fuchs, S. Paracrine effects influenced by cell culture medium and consequences on microvessel-like structures in cocultures of mesenchymal stem cells and outgrowth endothelial cells. *Tissue Eng Part A* **17**, 2199, 2011.
  39. Shi, Y., Kramer, G., Schröder, A., Kirkpatrick, C.J., Seekamp, A., Schmidt, H., and Fuchs, S. Early endothelial progenitor cells as a source of myeloid cells to improve the pre-vascularisation of bone constructs. *Eur Cell Mater* **27**, 64, 2014.
  40. Thébaud, N., Siadous, R., Bareille, R., Remy, M., Daculsi, R., Amédée, J., and Bordenave, L. Whatever their differentiation status, human progenitor derived–or mature–endothelial cells induce osteoblastic differentiation of bone marrow stromal cells. *J Tissue Eng Regen Med* **6**, e51, 2012.
  41. Dohle, E., Bischoff, I., Böse, T., Marsano, A., Banfi, A., Unger, R., and Kirkpatrick, C. Macrophage-mediated angiogenic activation of outgrowth endothelial cells in coculture with primary osteoblasts. *Eur Cell Mater J* **27**, 149, 2014.
  42. Dohle, E., Fuchs, S., Kolbe, M., Hofmann, A., Schmidt, H., and Kirkpatrick, C.J. Comparative study assessing effects of sonic hedgehog and VEGF in a human co-culture model for bone vascularisation strategies. *Eur Cell Mater* **21**, e56, 2011.
  43. Dohle, E., Fuchs, S., Kolbe, M., Hofmann, A., Schmidt, H., and Kirkpatrick, C.J. Sonic hedgehog promotes angiogenesis and osteogenesis in a coculture system consisting of primary osteoblasts and outgrowth endothelial cells. *Tissue Eng Part A* **16**, 1235, 2010.
  44. Herzog, D.P.E., Dohle, E., Bischoff, I., and Kirkpatrick, C.J. Cell communication in a coculture system consisting of outgrowth endothelial cells and primary osteoblasts. *Biomed Res Int* **2014**, 320123, 2014.
  45. Stahl, A., Wenger, A., Weber, H., Stark, G.B., Augustin, H.G., and Finkenzeller, G. Bi-directional cell contact-dependent regulation of gene expression between endothelial cells and

- osteoblasts in a three-dimensional spheroidal coculture model. *Biochem Biophys Res Commun* **322**, 684, 2004.
46. Xing, Z., Xue, Y., Finne-Wstrand, A., Yang, Z.Q., and Mustafa, K. Copolymer cell/scaffold constructs for bone tissue engineering: co-culture of low ratios of human endothelial and osteoblast-like cells in a dynamic culture system. *J Biomed Mater Res Part A* **101**, 1113, 2013.
  47. Deckers, M.M., Van Bezooijen, R.L., Van Der Horst, G., Hoogendam, J., van der Bent, C., Papapoulos, S.E., and Löwik, C.W. Bone morphogenetic proteins stimulate angiogenesis through osteoblast-derived vascular endothelial growth factor A. *Endocrinology* **143**, 1545, 2002.
  48. Au, P., Tam, J., Fukumura, D., and Jain, R.K. Bone marrow-derived mesenchymal stem cells facilitate engineering of long-lasting functional vasculature. *Blood* **111**, 4551, 2008.
  49. McFadden, T., Duffy, G., Allen, A., Stevens, H., Schwarzmaier, S., Plesnila, N., Murphy, J., Barry, F., Guldberg, R., and O'Brien, F. The delayed addition of human mesenchymal stem cells to pre-formed endothelial cell networks results in functional vascularization of a collagen-glycosaminoglycan scaffold in vivo. *Acta Biomater* **9**, 9303, 2013.
  50. da Silva Meirelles, L., Caplan, A.I., and Nardi, N.B. In search of the in vivo identity of mesenchymal stem cells. *Stem Cells* **26**, 2287, 2008.
  51. Leszczynska, J., Zyzynska-Granica, B., Koziak, K., Ruminski, S., and Lewandowska-Szumiel, M. Contribution of endothelial cells to human bone-derived cells expansion in coculture. *Tissue Eng Part A* **19**, 393, 2012.
  52. Hager, S., Lampert, F.M., Orimo, H., Stark, G.B., and Finkenzeller, G. Up-regulation of alkaline phosphatase expression in human primary osteoblasts by cocultivation with primary endothelial cells is mediated by p38 mitogen-activated protein kinase-dependent mRNA stabilization. *Tissue Eng Part A* **15**, 3437, 2009.
  53. Guillotin, B., Bareille, R., Bourget, C., Bordenave, L., and Amedee, J. Interaction between human umbilical vein endothelial cells and human osteoprogenitors triggers pleiotropic effect that may support osteoblastic function. *Bone* **42**, 1080, 2008.
  54. Kang, Y., Kim, S., Fahrenholtz, M., Khademhosseini, A., and Yang, Y. Osteogenic and angiogenic potentials of monocultured and co-cultured hBMSCs and HUVECs on 3D porous  $\beta$ -TCP scaffold. *Acta Biomater* **9**, 4906, 2013.
  55. Liu, Y., Teoh, S.H., Chong, M.S., Lee, E.S., Mattar, C.N., Randhawa, N.K., Zhang, Z.Y., Medina, R.J., Kamm, R.D., and Fisk, N.M. Vasculogenic and osteogenesis-enhancing potential of human umbilical cord blood endothelial colony-forming cells. *Stem Cells* **30**, 1911, 2012.
  56. Choi, M., Lee, H.-S., Naidansaren, P., Kim, H.-K., Eunju, O., Cha, J.-H., Ahn, H.-Y., Yang, P.I., Shin, J.-C., and Joe, Y.A. Proangiogenic features of Wharton's jelly-derived mesenchymal stromal/stem cells and their ability to form functional vessels. *Int J Biochem Cell Biol* **45**, 560, 2013.
  57. Verseijden, F., Posthumus-van Sluijs, S.J., Pavljasevic, P., Hofer, S.O., van Osch, G.J., and Farrell, E. Adult human bone marrow- and adipose tissue-derived stromal cells support the formation of prevascular-like structures from endothelial cells in vitro. *Tissue Eng Part A* **16**, 101, 2009.
  58. Takahashi, M., Suzuki, E., Oba, S., Nishimatsu, H., Kimura, K., Nagano, T., Nagai, R., and Hirata, Y. Adipose tissue-derived stem cells inhibit neointimal formation in a paracrine fashion in rat femoral artery. *Am J Physiol Heart Circ Physiol* **298**, H415, 2010.
  59. Bronckaers, A., Hilkens, P., Fanton, Y., Struys, T., Gervois, P., Politis, C., Martens, W., and Lambrechts, I. Angiogenic properties of human dental pulp stem cells. *PLoS One* **8**, e71104, 2013.
  60. Burlacu, A., Grigorescu, G., Rosca, A.-M., Preda, M.B., and Simionescu, M. Factors secreted by mesenchymal stem cells and endothelial progenitor cells have complementary effects on angiogenesis in vitro. *Stem Cells Dev* **22**, 643, 2012.
  61. Villars, F., Bordenave, L., Bareille, R., and Amedee, J. Effect of human endothelial cells on human bone marrow stromal cell phenotype: role of VEGF? *J Cell Biochem* **79**, 672, 2000.
  62. Choi, K.D., Yu, J., Smuga-Otto, K., Salvaggio, G., Rehrauer, W., Vodyanik, M., Thomson, J., and Slukvin, I. Hematopoietic and endothelial differentiation of human induced pluripotent stem cells. *Stem Cells* **27**, 559, 2009.
  63. Rufaihah, A.J., Huang, N.F., Kim, J., Herold, J., Volz, K.S., Park, T.S., Lee, J.C., Zambidis, E.T., Reijo-Pera, R., and Cooke, J.P. Human induced pluripotent stem cell-derived endothelial cells exhibit functional heterogeneity. *Am J Transl Res* **5**, 21, 2013.
  64. Spicer, P.P., Kretlow, J.D., Young, S., Jansen, J.A., Kasper, F.K., and Mikos, A.G. Evaluation of bone regeneration using the rat critical size calvarial defect. *Nat Protoc* **7**, 1918, 2012.

Address correspondence to:

*Ping Wang, DDS, PhD*  
*Department of Endodontics, Periodontics*  
*and Prosthodontics*  
*University of Maryland School of Dentistry*  
*Baltimore, MD 21201*

*E-mail: dentistping@gmail.com*

*Liang Zhao, MD, PhD*  
*Department of Orthopedic Surgery*  
*Nanfang Hospital*  
*Southern Medical University*  
*Guangzhou*  
*Guangdong 510515*  
*China*

*E-mail: lzhaonf@126.com*

*Chongyun Bao, DDS, PhD*  
*State Key Laboratory of Oral Diseases*  
*West China Hospital of Stomatology*  
*Sichuan University*  
*Chengdu*  
*Sichuan 610041*  
*China*

*E-mail: cybao9933@yahoo.com.cn*

*Received: November 7, 2016*

*Accepted: January 27, 2017*

*Online Publication Date: March 10, 2017*